The Human Amyloid Precursor Protein Binds Copper Ions Dominated by a Picomolar Affinity Site in the Helix-Rich E2 Domain

Tessa R. Young,[†] Tara L. Pukala,[‡] Roberto Cappai,[§] Anthony G. Wedd,[†] and Zhiguang Xiao[*,†,¶]

[†] School of Chemistry and Bio21 Molecular Science and Biotechnology Institute, The University of Melbourne, Parkville, Victoria 3010, Australia.

[‡] School of Chemistry and Physics, The University of Adelaide, Adelaide, SA 5005, Australia.

[§] Department of Pharmacology and Therapeutics, The University of Melbourne, Parkville, Victoria 3010, Australia.

[¶] Melbourne Dementia Research Centre, Florey Institute of Neuroscience and Mental Health, The University of Melbourne, Parkville, Victoria 3052, Australia

ABSTRACT: A manifestation of Alzheimer's disease (AD) is the aggregation in the brain of amyloid β (Aβ) peptides derived from the amyloid precursor protein (APP). APP has been linked to modulation of normal copper homeostasis while dysregulation of Aβ production and clearance has been associated with disruption of copper balance. However, quantitative copper chemistry on APP is lacking, in contrast to the plethora of copper chemistry available for Aβ peptides. The soluble extracellular protein domain sAPPα (molar mass including post-translational modifications ~ 100 kD) has now been isolated in good yield and high quality. It is known to feature several copper binding sites with different affinities. However, under copper-limiting conditions, it binds either Cu(I) or Cu(II) with picomolar affinity at a single site (labeled M1) that is located within the APP E2 subdomain. M1 in E2 was identified previously by X-ray crystallography as a Cu(II) site that features four histidine side-chains (H313, H386, H432, H436) as ligands. The presence of $Cu^{II}(His)_4$ is confirmed in solution at pH ≤ 7.4 while Cu(I) binding involves either the same ligands or a subset. The binding affinities are pH-dependent and the picomolar affinities for both Cu(I) and Cu(II) at pH 7.4 indicate that either oxidation state may be accessible under physiological conditions. Redox activity was observed in the presence of an electron donor (ascorbate) and acceptor (dioxygen). A critical analysis of the potential biological implications of these findings is presented.

INTRODUCTION

The amyloid precursor protein (APP) is implicated in Alzheimer's disease (AD) due to the abundance of its amyloid beta (Aβ) peptide products in the plaques present in AD brain tissues.[1-2] Aβ fragments (< 42 amino acids) are produced, along with a soluble extracellular product sAPPβ, from sequential proteolysis of APP by β- and γ-secretases in the 'amyloidogenic' processing pathway (Figure 1). Alternative 'non-amyloidogenic' processing by α-secretase releases soluble sAPPα without resultant Aβ production.[3]

AD is associated with disruptions in the homeostasis of several metal ions including copper.[4] Locally elevated copper levels have been reported within Aβ plaques[5-6] and decreased levels in surrounding brain tissues.[7-8] *In vitro* experiments show that interactions between Cu and Aβ can cause peptide aggregation and generate toxic reactive oxygen species (ROS) via the Cu(II)/Cu(I) redox couple; if such interactions occur *in vivo*, they could be a source of neuronal damage.[9] On the other hand, Cu deficits in nonplaque brain regions may diminish the activity of vital enzymes such as superoxide dismutase (SOD1) that could also contribute to neurotoxicity.[10]

Chelating ligands have been tested as potential therapeutics to extract weakly-bound metals from extracellular amyloid plaques and to redistribute them to their correct intracellular destinations, thereby restoring metal homeostasis.[11-12] However, despite promising initial results, candidates failed clinical trials for AD.[13]

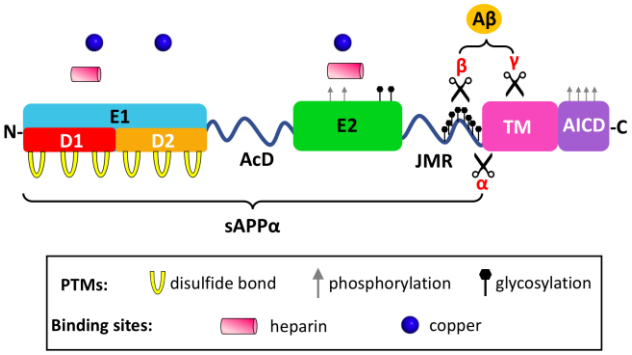

Figure 1. Schematic representation of the overall structure and subdomains of APP_{695} (molar mass of the primary sequence: 67.7 kDa) showing cleavage sites for amyloidogenic (β and γ) and non-amyloidogenic (α and γ) processing pathways. Known post-translational modifications (PTMs) are indicated (disulfide bonds, phosphorylation and glycosylation sites), as are known heparin and Cu binding sites (see inset for key).

The reasons are unclear but may be due to misunderstanding the inorganic chemistry at play.[14] Important questions remain unanswered, including: Do metal ions really interact meaningfully with cellular APP? If so, are these interactions functional or pathogenic? Answers may guide design of sensible, targeted strategies for disease intervention.

Cumulative biological evidence documents correlations between APP and cellular copper homeostasis. Copper accumulates intracellularly in APP knockout, particularly in liver and brain tissues.[15-16] Increases in the cellular copper level upregulate APP gene expression and vice-versa.[17-18] Cu affects APP processing and Aβ production: elevated copper levels promote the non-amyloidogenic pathway, while cellular copper deficiency enhances amyloidogenic processing.[10, 19-20] APP displays Cu-responsive trafficking behavior and redistributes from intracellular compartments to the plasma membrane in response to high copper levels.[21] This latter process resembles that of the transmembrane copper pump ATP7A.[22-23] While there clearly appears to be a biological link between copper and APP, it is unclear whether it is a consequence of direct metal-protein interactions.

Multi-domain protein APP exists in several spliced isoforms. The shortest form expressed at high levels in the brain is APP_{695} that features a large ectodomain, a single-pass transmembrane domain TM and a small intracellular domain AICD (Figure 1). The ectodomain includes two structured domains E1 (encompassing interacting subdomains D1 and D2) and E2 that are connected by a flexible acidic domain AcD. A juxtamembrane region JMR links the extracellular protein to TM.

The mature protein contains significant post-translational modifications including six structural disulfide bonds in the E1 domain[24-26] and numerous phosphorylation and glycosylation sites that may be involved in regulation of protein function (Figure 1).[27] Two heparin-binding sites[28-30] mediate interactions between APP and extracellular matrix proteins[28, 31] and promote APP homo-dimeriation.[26, 32-33] These properties are linked to APP's proposed function as a cell adhesion molecule.[3, 34]

Employing crystals soaked in excess Cu_{aq}^{2+}, three Cu(II) binding sites were identified in isolated domains of APP by X-ray crystallography (Figure 2).[25, 35-37] There are two in domain E1 (one each in subdomains D1 and D2) and a third in domain E2 (M1 site). Each employs histidine ligands primarily. As the site in D2 was identified first,[38] it is commonly referred to as the 'copper binding domain' (CuBD).[25] Ligand competition experiments have revealed that D2 can bind Cu(I) with approximately 100-fold stronger affinity ($K_D \sim 10^{-10}$ M) than Cu(II) ($K_D \sim 10^{-8}$ M).[39] This highlights the importance of considering both oxidation states. APP E2 was demonstrated to bind Cu(I) with picomolar (pM) affinity when bound to its biological ligand heparin.[40]

However, a robust thermodynamic comparison of Cu binding for each of the identified sites in Figure 2 and other possible unidentified sites in the whole ectodomain sAPPα is not available. Fundamental questions remain as to (i) which is the preferred binding site(s); (ii) which is the preferred metal oxidation state; (iii) whether the Cu-binding interactions of the complete ectodomain sAPPα differ from those of isolated individual subdomains (due to, for example, cooperative binding) and (iv) whether Cu binding affinities of APP are sufficiently strong to compete with extracellular Cu-binding proteins such as human serum albumin (HSA) or the high-affinity Cu transporter (Ctr1).

In this work, the ectodomain sAPPα and its subdomains have been isolated in high yield and purity. With the availability of probes developed recently for quantification of the interactions of both Cu(I) and Cu(II) with biomolecules,[41-42] this has enabled a comprehensive thermodynamic analysis of the interactions between APP domains and copper ions. sAPPα binds *either* Cu(I) or Cu(II) with picomolar affinity at the tetra-His M1 site in domain E2. Binding of copper to this site results in protein structural change and redox activity that are modulated by biological partners of APP, including heparin.

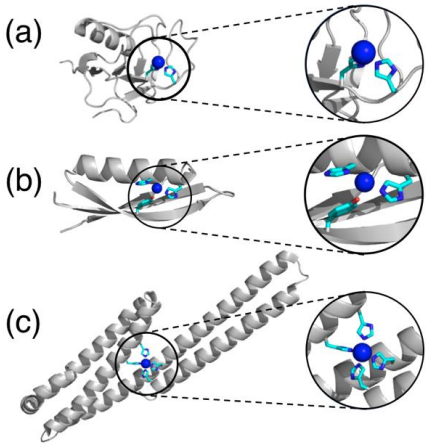

Figure 2. Structures of APP subdomains with bound Cu(II) ions: (a) D1 ligands H108 and H110 (PDB: 4JFN); (b) D2 ligands H147, H151 and possibly Y168 (PDB 2FK1); (c) E2 ligands H313, H382, H432 and H436 (PDB 3UMK).

RESULTS

Expression, purification and characterisation of APP domains

The complete extracellular domain sAPPα (residues 18-611) of APP and the separate subdomains D1 (28-123), D2 (133-189) and E1 (28-189) were expressed and purified from transformed *Pichia pastoris* cells by adapting published procedures with an extra final step of size-exclusion chromatography in each case to ensure highest sample purity. Details are provided in the Supporting Information sections 3-7 (SI 3-7). APP E2 (295-498) and two variants AcE2 and AcE2-qm were expressed and purified from transformed *Escherichia coli* cells as reported previously.[40] AcE2 has the N-terminal amine blocked by acetylation and AcE2-qm also has the four His residues (His-313, 382, 432, 436) that define the M1 site replaced by Ala. Purities were confirmed by sodium dodecyl sulfate-polyacrylamide gel electrophoresis and ultraviolet-visible spectroscopy (Figures S1 and S2). Identities were verified by electrospray ionization mass spectrometry (ESI-MS) except for sAPPα (Table 1). The latter was produced with heterogeneous *P. pastoris*-derived PTMs (including glycosylations) that compromised the resolution of ESI-MS spectra; its identity was verified by proteolytic digestion and peptide mapping (see SI 7 and Figures S3 and S4).

Cu(I) binding in sAPPα is dominated by the M1 site in the E2 domain

The affinities for Cu(I) of extracellular APP domains with single (D1, D2, E2) or multiple (E1, sAPPα) His-rich sites were evaluated under a unified affinity scale. The analysis was performed via competition for Cu(I) with probe ligands L = Ferene S (Fs), Ferrozine (Fz) and Bicinchoninate (Bca) that form chromophoric $[Cu^{I}L_2]^{3-}$ anions in the presence of excess ligand (see Table S1).[41, 43]

Table 1. Characterisation data of isolated APP domains

Protein domain	APP_{695} residues	Molar mass (Da)		ε_{280} ($cm^{-1}\ M^{-1}$)[a]
		Found	Expected	
D1[b]	28-123	11233	11234	15,845
D2[b]	133-189	6832	6833	7,365
E1[b]	28-189	18786	18786	23,210
E2[c]	295-498	25385	25386	15,930
AcE2[c]	298-498	25427	25428	15,930
AcE2-qm[c,d]	295-498	25162	25163	15,930
sAPPα[e]	18-611	n/a[f]	n/a[f]	60,110

[a] Calculated from protein sequences; [b] Including extra N-terminal residues EA from the expression vector pPIC9; [c] Including extra N-terminal residues MN and C-terminal residues GSENLYFQ from a modified pET20b vector (see ref [40]); [d] Including four His to Ala point mutations (H313,382,432,436A) corresponding to the M1 metal-binding site; [e] Including extra N-terminal residues REFPGM from the expression vector pHIL-S1; [f] Variable protein masses as a result of heterogeneous post-translational modifications. Identity confirmed by trypsin digestion and peptide mapping, see ESI 6-7 and Figures S2-4.

The Cu(I) binding properties of subdomains D1 and D2 (Figures 1 and 2) were characterized separately with Fs, the lowest affinity ligand of the set, in a solution buffered at $p[Cu^+] = -\log[Cu^+] = 8.2$ (Figure S5a and Table S1). A Cu(I)-binding stoichiometry of 1:1 for each subdomain was established. Fitting of the experimental data to a single binding site model (see SI 10) provided log $K_D \sim -10$ for each subdomain, consistent with a previous estimate for D2 (Table 2).[39]

The complete E1 domain (containing subdomains D1 and D2) bound, as expected, two equivalents (equiv) of Cu(I) (Figure 3a). Competition experiments employing either ligand Fs or Fz fitted well to a model of two separate Cu(I) sites of equivalent affinity and derived an average log $K_D = -10.2$ for each of the sites at physiological pH (Figures 3a and Figure S5b). It is apparent that E1 binds two Cu(I) ions with nanomolar affinity and no cooperativity.

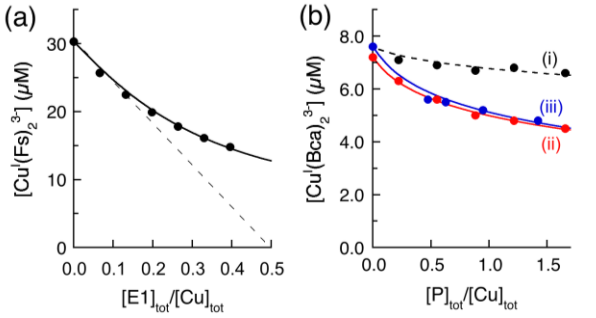

Figure 3. Quantification of Cu(I) binding affinities. (a) Changes in concentrations of $[Cu^I(Fs)_2]^{3-}$ in solution ($[Cu(I)]_{tot}$ = 30.3 μM; $[Fs]_{tot}$ = 70 μM) as a function of increasing concentrations of APP E1 domain; (b) Changes in concentrations of $[Cu^I(Bca)_2]^{3-}$ in solution ($[Cu(I)]_{tot}$ = 7.2 μM; $[Bca]_{tot}$ = 16.6 μM) as a function of increasing concentrations of E1 (i), E2 (ii) and sAPPα (iii) in the presence of one equiv of heparin H3393 (relative to protein). The solid traces show fitting of the experimental data to a model of two identical binding sites for E1 in (a) and of one binding site for E2 and sAPPα in (b) (see ESI 10 for details). The derived affinity data (expressed as log K_D) are listed in Table 2. The dotted trace (i) in (b) is a simple interpolation of the experimental data for E1 since its competition for Cu(I) with ligand Bca was too weak to allow a meaningful affinity estimation. All experiments were conducted in Mops buffer (50 mM, pH 7.4) under reducing conditions (1.0 mM NH_2OH, 0.5 mM Asc). The competition experiments with probe Bca also contained 100 mM NaCl.

A complication arises as the E2 domain forms ternary complexes E2-Cu(I)-L in the presence of probe ligands L = Fs, Fz and Bca, preventing Cu(I) affinity determination via the competition experiments.[40] However, as demonstrated recently, these ternary complexes are disrupted in the presence of heparin, an established physiological partner of APP. This allowed a reliable estimation of the Cu(I) affinity of the heparin-bound APP E2: log $K_D = -12.1$ at pH 7.4.[40] This picomolar affinity is lost for the protein variant APP E2-qm in which the four His ligands in the M1 site are replaced by Ala.[40]

The ectodomain sAPPα (containing E2) shows equivalent behavior: it forms a ternary complex with Cu(I) and ligand Bca in the absence of heparin but not in its presence (see SI 8 and Figure S6). Consequently, the highest Cu(I) binding affinities of domains E1, E2 and sAPPα were evaluated and compared via competition for Cu(I) with higher affinity ligand Bca in the presence of heparin (Figure 3b and Figure S5c). Under such conditions, the Cu(I) binding is limited to the highest affinity site only in each protein. The Cu(I) binding curve of sAPPα superimposed that of E2 and the affinity was much higher than that of E1 (Figure 3b). High affinity Cu(I) binding in sAPPα is dominated solely by the M1 site in E2. The sites of nanomolar affinity in E1 cannot compete.[44]

The presence of heparin had no detectable impact on Cu(I) binding to D2, but appeared to double the affinity of D1 and, consequently, E1 (Table 2). APP D1, but not D2, is known to interact with heparin.[28]

Table 2. Cu binding affinities of APP domains and related proteins at pH 7.4

Protein	Heparin present?	Cu(I) affinity		Cu(II) affinity	
		log K_D[a]	probe	log K_D	probe
APP domains					
sAPPα	x			−11.4	DP3
	√	−11.9	Bca	−11.4	DP3
E1[b]	x	−10.2	Fs/Fz	−8.3	DP1
	√	−10.4	Fs/Fz	ND[c]	
D1	x	−10.0	Fs	−8.1	DP1
	√	−10.4	Fs		
D2	x	−10.0	Fs	−8.1	DP1
	√	−10.0	Fs		
	x	−10.1[d]	Fs		
E2	x			−11.4	DP3
	√	−11.9	Fz		
AcE2	x			−11.4	DP3
	√	−11.9	Bca	−11.4	DP3
	√	−12.1[e]	Bca/Fz		
AcE2qm	x			> −8.3[d]	DP1
	√	> −11.0[e,f]	Fz		
Extracellular Cu-binding proteins					
HSA	x			−12.7	DP3
	x			−12.0[g]	
Ctr1n	x	−12.8[h]		−11.0[h]	

[a] Where more than one probe was used, an average log K_D was taken. [b] Assuming 2 Cu sites of equal affinity. [c] Not determined quantitatively due to comparable weak Cu(II) affinity of heparin. [d] Ref [39]. [e] Ref [40]. [f] Adventitious binding/potential interference from more than one metal binding site was observed, only an upper affinity limit is given. [g] From ref [45]. [h] From ref [46].

Cu(II) binding in sAPPα is dominated by the M1 site in the E2 domain

To complement the Cu(I) binding studies, Cu(II) binding to sAPPα and its subdomains was quantified with a set of three complementary fluorescent dansyl peptide probes (DP1-3).[42] These probes fluoresce at λ_{max} = 550 nm upon excitation at 330 nm but Cu(II) binding induces linear quenching (Figure 4a). They each bind one equiv of Cu(II) with different affinities (Table S2) and this allows quantification of Cu(II) binding stoichiometry and affinity.

The DP1 probe was employed first for its weaker affinity (log K_D = –8.1 at pH 7.4).[42] A control titration of $CuSO_4$ into a solution of *apo*-DP1 (2.0 μM) in Mops buffer (5.0 mM, pH 7.4, 100 mM NaCl) induced linear fluorescence quenching with an endpoint at Cu/DP1 ~ 1 (Figure 4b(i)). Equivalent titrations in the presence of one equiv of APP E1, E2 and sAPPα generated titration curves (ii), (iii) and (iv), respectively (Figure 4b). Curve (ii) for E1/DP1 had no clear endpoint, but suggested that E1 competes for Cu(II) with comparable affinity to DP1 and can apparently bind ~ 3 equiv of Cu(II) with contributions from weak binding sites. In contrast, the titration curve (iii) for E2/DP1 showed little fluorescence quenching until addition of one equiv of Cu^{2+} with a sharp turning point. The behavior indicated that E2 features a distinct high affinity Cu(II) binding site that outcompetes DP1. sAPPα features the full length soluble extracellular domain including E1, E2 and other subdomains (Figure 1). Consequently, the titration curve (iv) for sAPPα/DP1 was more than the sum of (ii) for E1 and (iii) for E2, due to the sensitivity of the DP1 probe to weak Cu(II) binding.

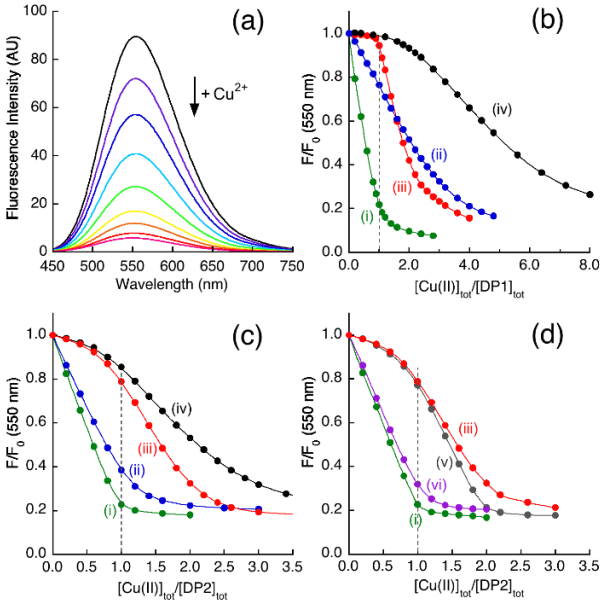

Figure 4. Analysis of Cu(II) binding to APP domains with DP probes in Mops buffer (5.0 mM, pH 7.4, 100 mM NaCl). (a) Typical fluorescence quenching response of a DP probe to Cu(II) binding (λ_{ex} = 330 nm; λ_{em} = 550 nm); (b-d) Cu^{2+} titration curves for probes DP1 (b) and DP2 (c, d) in the presence of: (i, green) a DP probe (2.0 μM) only; (ii-vi) a 1:1 mixture (each 2.0 μM) of a DP probe and an APP domain of E1 (ii, blue), E2 (iii, red), sAPPα (iv, black), AcE2 (v, grey) and AcE2-qm (vi, violet). The solid traces are the simple interpolations of the experimental data.

The higher affinity probe DP2 (log K_D = -10.1 at pH 7.4)[42] was employed next for the equivalent experiments (Figure 4c, d) that led to the following observations and conclusions:-

(1) Titration curve (ii) for E1/DP2 was similar to control titration (i) for DP2 alone, indicating that DP2 outcompetes the entire E1 domain and that the latter does not contain a Cu(II) binding site with subnanomolar affinity;

(2) Titration curves (iii) for E2/DP2 and (iv) for sAPPα/DP2 showed similar behavior, contrasting with their different behavior with probe DP1 (compare Figure 4c and 4b); the observations indicate that there are extra low affinity binding sites in sAPPα;

(3) Titration curve (iii) for E2/DP2 differed only marginally from (v) for AcE2/DP2, but dramatically from (vi) for AcE2-qm. AcE2 lacks a free N-terminal amine that can make a minor contribution only to the weaker Cu(II) binding. On the other hand, the behavior of AcE2-qm (lacking His-313, 382, 432, 436) identifies the tetra-His M1 site as the high affinity Cu(II) binding site in E2.

To minimize complications from binding of multiple Cu(II) ions, the highest affinity site of each APP domain was evaluated quantitatively by titration of the metal-free APP domain into a suitable Cu^{II}-DP complex in the presence of a slight excess of the *apo*-DP probe. Competitive transfer of Cu(II) from Cu^{II}-DP to the APP domain was monitored by recovery of the probe fluorescence intensity and the affinity estimated from Cu(II) speciation analysis of the titration data (see ESI 11 for details). DP3 (log K_D = -12.1 at pH 7.4)[42] proved to be ideal for the purpose. Titration of a selected APP domain into a solution of $Cu^{II}_{0.8}$-DP3 (2.0 μM) in Mops buffer (50 mM, pH 7.4, 100 mM NaCl) generated titration curves (i), (ii), (iii) in Figure 5a for E1, E2 and sAPPα, respectively. Curves (ii) for E2 and (iii) for sAPPα superimposed, with the probe fluorescence intensity recovering as the titration proceeded. This confirmed the existence of the same high affinity Cu(II) binding M1 site in each and the lack of binding cooperativity between the M1 site and other weaker Cu(II) binding sites. A quantitative correlation of [Cu^{II}-DP3] versus [protein]$_{tot}$/[DP3]$_{tot}$ estimated log K_D = –11.4 at pH 7.4 for the M1 site (Figure 5b; see ESI 11 for details).

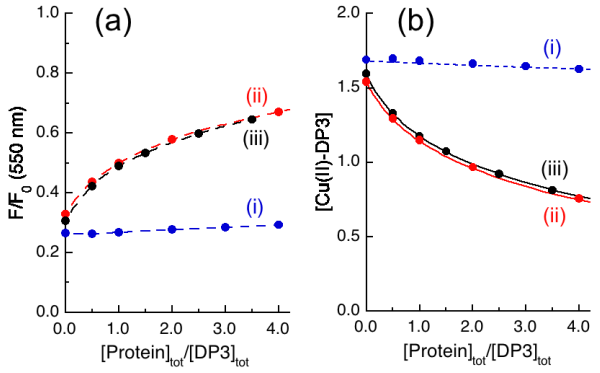

Figure 5. Determination of the conditional log K_D of the highest affinity site for Cu(II) in APP E2 and sAPPα with probe DP3: (a) Recovery of DP3 fluorescence intensity upon titration of proteins E1 (i), E2 (ii) and sAPPα (iii) into a solution of $Cu^{II}_{0.8}$-DP3 (2.0 μM) in Mops (50 mM, pH 7.4, 100 mM NaCl); (b) Correlation of [Cu^{II}-DP3] with [protein]$_{tot}$/[DP3]$_{tot}$ ratio for each set of experimental data in (a). The solid traces show the best fitting of the experimental data to a one site binding model. The derived affinity data are summarised in Table 2. APP E1 does not compete for Cu(II) with the DP3 probe effectively (traces i).

In contrast, the flat titration curve (i) for APP E1 was consistent with little competition with higher affinity probe DP3. Further experiments with weaker probe DP1 (Figure S7) provided indistinguishable nanomolar Cu(II) affinities for E1, D1

and D2 (log K_D = ~ –8.2 at pH 7.4; Table 2) that matched those of previous estimates.[37, 39] Again, no cooperativity between D1 and D2 was detected.

Control experiments demonstrated that heparin has no impact on the Cu(II) binding to the high affinity M1 site in E2 or sAPPα (Table 2). Binding of Cu(II) to E1 remained weak in the presence of heparin.

In conclusion, the only Cu(II) binding site of picomolar affinity in the entire ectodomain sAPPα is the M1 site within the E2 domain.

Competition for Cu(II) between E2 and human serum albumin

The pK_a of a free His side-chain is about 6.0. The pH dependence of the affinity of the tetra-His M1 site for Cu(II) in E2 in the range pH 5.6-7.4 (black circles in Figure 6a) is indistinguishable with that of sAPPα (red crosses). DP3 was the detection probe under the conditions of Figure 5. The data can be fitted (black line) assuming a single tetra-His M1 site (Figure 6b; ESI 11), providing pK_D = –log K_D = 11.2 (pH-independent) and an average pK_a = 6.4 for the four His ligands. This interpretation is again consistent with a dominant tetra-His M1 site in sAPPα at pH < 7.4 with little, if any, contribution from lower-affinity sites.

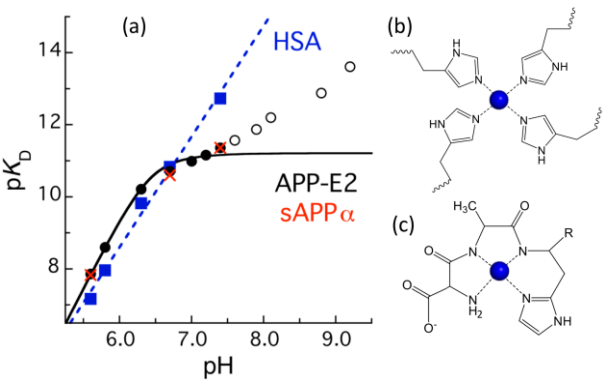

Figure 6. (a) Variation of conditional pK_D (= −log K_D) with solution pH for APP-E2 (black filled and empty circles), sAPPα (red crosses) and HSA (blue squares) over the pH range 5.6 – 9.2. The solid trace corresponds to curve-fitting of the experimental data of E2 at pH < 7.4 to a tetra-His site model shown in (b), generating log K_D = –11.2 at pH > 7 and an average pK_a = 6.4 for the four His ligands (see ESI 11). The experimental data for E2 at pH > 7.4 (open circles) deviated from the model and were excluded from the curve fitting. The dotted trace corresponds to simple interpolation of the pH-dependent data for HSA which features an ATCUN binding site shown in (c) for its N-terminal Asp-Ala-His sequence.

However, the pH dependence of the apparent pK_D for E2 increased at pH > 7.4 (Figure 6a, open circles) in a way that could not be fitted with the tetra-His M1 model. The Cu^{II}-E2 EPR spectrum also changes (Figure S8) in a way consistent with the presence of an anionic amide ligand(s) induced by deprotonation of backbone peptide linkages. The behavior was not characterized further as it occurred outside the physiologically meaningful pH range.

Can the M1 site compete with putative extracellular Cu(II)-binders such as human serum albumin (HSA) and the extracellular domain of the high affinity Cu importer Ctr1? Both HSA and Ctr1 feature an 'amino terminal Cu(II)- and Ni(II)-binding' (ATCUN; Figure 6c) site that may play roles in Cu(II) binding and transport. The Cu(II) binding affinities of HSA in the pH range 5.6-7.4 were estimated using the DP3 probe following the same protocol used for APP E2 (Figure 6a, blue squares). An estimate of log K_D = –12.7 at pH 7.4 was obtained, comparable to a value of –12.0 reported previously (Table 2).[45] Thus, thermodynamically, a competition between HSA and sAPPα for binding Cu(II) ions is expected, with HSA binding more favorably at pH 7.4.

However, the pH-dependence of the binding affinities of the two systems differ as a result of the different ligands involved in each site (Figure 6b, c). The conditional affinity data shown in Figure 6a indicate that the Cu(II) dissociation constants for E2 and HSA are the same at pH ~ 6.7. At pH > 6.7, HSA has the higher affinity while, at pH < 6.7, E2 does.

This finding was verified by metal speciation analysis via direct competition for limiting Cu(II) between E2 and HSA using EPR as a detection probe (Figure 7). Control experiments showed that the EPR spectra of Cu(II)-E2 and Cu(II)-HSA were distinct and changed little within the pH range 6.2 – 7.4 (Figure S9). Therefore, the spectra of equimolar solutions of E2 and HSA under Cu(II) limiting conditions independently confirm the relative affinities of the two Cu(II) binding proteins (Figures 6 and 7). It is again apparent that at pH > 6.7, HSA has the higher affinity while, at pH < 6.7, E2 does.

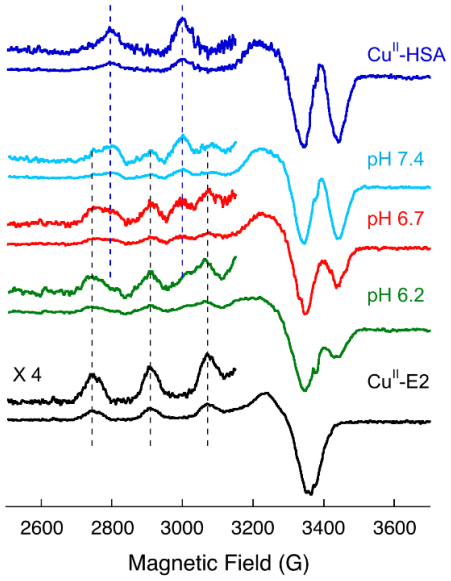

Figure 7. Frozen solution EPR spectra recorded at 77 K probing the coordination environment of Cu(II) ions (120 μM) in mixtures of E2 and HSA (150 μM each) at selected pH = 6.2, 6.7 and 7.4. Control spectra for Cu^{II}-E2 and Cu^{II}-HSA are shown for comparison. Solutions were prepared in 50 mM buffer (Mes pH 6.2-6.7; Mops pH 7.4) with 500 mM NaCl and 10 % glycerol.

The different nature of the Cu(II) binding sites in E2 and HSA suggest that the rate of their reactions with Cu(II) may differ. Transfer of Cu(II) between E2 and DP3 was much faster than that between HSA and DP3 under the same conditions (Figure S10), consistent with the known slow kinetics of Cu(II) binding to and dissociation from the ATCUN site.[42, 47]

Cu(II) binding stabilises the structure of E2 and alters its conformation

The impact of Cu(II) binding on the stability and conformation of E2 can be evaluated by ESI-MS. A folded structure in the gas phase minimizes surface protonation and is characterized by low

charge ions with a narrow m/z distribution. Protein unfolding leads to higher surface exposure and to high charge ions with a broader m/z distribution.[48]

The native ESI-MS mass spectrum of *apo*-E2 displayed a bimodal charge-state distribution encompassing both high and low m/z values (Figure 8). In contrast, the m/z distribution of Cu(II)-E2 was dominated by ions of lower charge. Inhibition of protein unfolding is a consequence of Cu(II) binding.

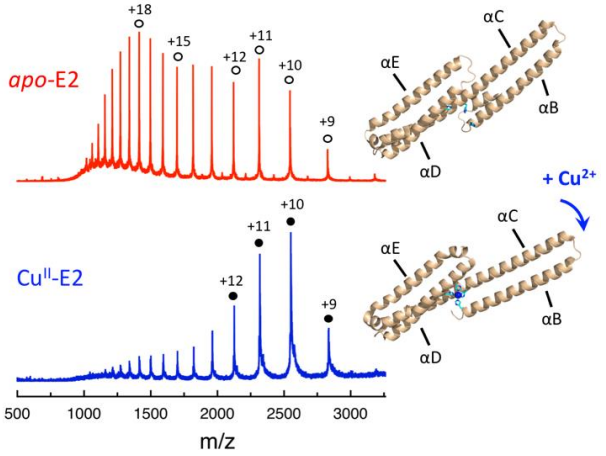

Figure 8. Native ESI-MS of *apo*-E2 and Cu^{II}-E2. Selected charge states of *apo*- (○) and Cu^{II}-bound (●) domain are indicated. Inset: cartoon presentations of X-ray crystal structures for *apo*-E2 (PDB: 3NYL) and Cu^{II}-E2 (PDB: 3UMK). Side-chains of the four Cu(II)-coordinating His residues (H313,382,432,436) from helices B, C and D are shown in sticks and the bound Cu(II) ion as a blue sphere.

Table 3. Experimental and calculated CCSs for *apo*- and Cu^{II}-E2 (Å^2)

Protein	Exptl CCS (charge state indicated) [a]				Calced CCS
	9+	10+	11+	12+	
apo-E2	2077	2057	2154	2473/2892	1996 [b]
Cu^{II}-E2	2195	2190	2311	2538	2145 [c]

[a] The E2 protein isolated in this work contained 31 more residues than the resolved X-ray structure of the sequence APP309-491 used for the calculation and this may contribute to the marginally higher experimental values than the calculated ones; [b] Calculated from reported *apo*-E2 structure (PDB: 3NYL); [c] Calculated from reported Cu^{II}-E2 structure (PDB: 3UMK).

Ion mobility-mass spectrometry (IM-MS) is able to distinguish different protein conformations in ions of the same charge by comparing arrival time distributions (ATD) and the corresponding collision cross sections (CCS).[49] A detailed analysis is presented in Figure S11 and Table 3 with the conclusions:

(i) Higher charge *apo*-E2 ions are partially unfolded;

(ii) Lower charge *apo*- and Cu^{II}-E2 ions are essentially folded.

Notably, the experimental CCS values of the folded *apo*-E2 were significantly smaller than those of the Cu(II)-bound form (Table 3), indicating that Cu(II) binding leads to expansion of the E2 structure. X-ray crystallography revealed that Cu(II) binding to the M1 site of *apo*-E2 induces rotation of helices αB and αC to a more open structure (compare the two structures in Figure 8).[36]

CD spectra indicated that Cu(II) binding to the M1 site increased the α-helical content of E2 slightly but consistently (Figure S12), as also observed previously.[36]

In summary, Cu(II) binding to the M1 site stabilizes the structure of E2 and alters the structural conformation to a more rigid but more open state.

Redox catalysis of the Cu-E2 complex

The tetra-His M1 site in APP E2 is the highest affinity location for both Cu(I) and Cu(II) ions in sAPPα. Given that these affinities are similar (Table 2), either oxidation state should be accessible under physiological conditions. On the basis of these affinities, the Nernst equation predicts a reduction potential of approximately +190 mV for the Cu-M1 center, a value intermediate between those for ascorbate (Asc) oxidation (approximately +50 mV)[50] and dioxygen reduction (approximately + 300 mV)[51] at neutral pH (Figure 9a). Consequently, the center should be redox-active in catalyzing dioxygen oxidation of Asc, an antioxidant abundant in the central nervous system.[52] Under anaerobic conditions, Asc reduced the Cu(II)-E2 complex to the Cu(I)-form completely, as confirmed by the loss of EPR signal of the Cu(II)-M1 center (Figure 9b). However, in an aerobic buffer, Asc was oxidized catalytically in the presence of Cu(II)-E2 (Figure 9c). Asc was stable in the same buffer containing *apo*-E2 without Cu. The oxidation rate was proportional to Cu concentration in the presence of excess *apo*-E2 (Figure 9d), consistent with the Cu-E2 complex as a catalyst for the oxidation.

The catalytic reaction is more complex than that represented in Figure 9a and is known to produce 1e$^-$ (superoxide) and 2e$^-$ (peroxide) examples of reactive oxygen species (ROS). Redox cycling led to oxidation of APP E2: mass spectra detected ions at 16 amu intervals, corresponding to sequential additions of oxygen atoms (Table 4 and Figure 10). Controls lacking Cu and/or reductant Asc showed minimal oxidation. In the presence of heparin, catalysis also occurred but with a ~50% reduction in the oxidation rate and lower levels of protein oxidation. Upon addition of ligand Bca, the reaction was silenced and protein oxidation suppressed, consistent with trapping of Cu(I) as the stable ternary complex E2-Cu(I)-Bca.[40]

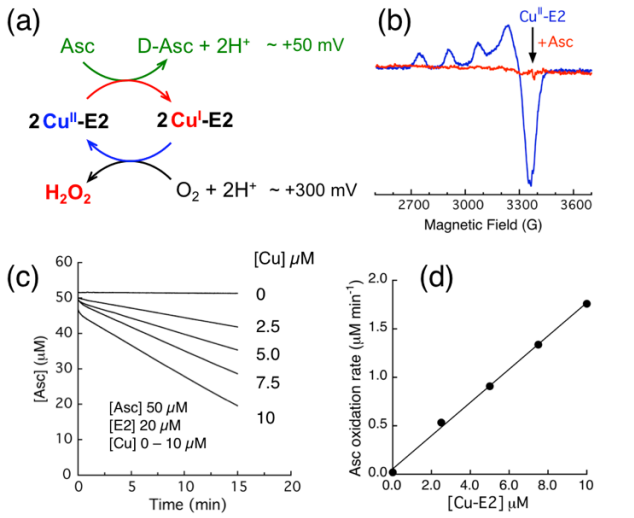

Figure 9. Redox activity of the Cu-E2 complex. (a) Scheme for aerobic catalytic oxidation of Asc. (b) Reduction of the complex (200 μM) by Asc (2.0 mM) at pH 7.4 under anaerobic conditions, monitored by EPR spectroscopy. (c) Observed change in Asc concentration over time (monitored by absorbance at 265 nm) in solutions of *apo*-E2 (20 μM) in Mops buffer (50 mM, pH 7.4, 100 mM NaCl) containing 0-10 μM Cu (added as $CuSO_4$). (d) Asc oxidation rate from (c) plotted as a function of the Cu-E2 complex concentration.

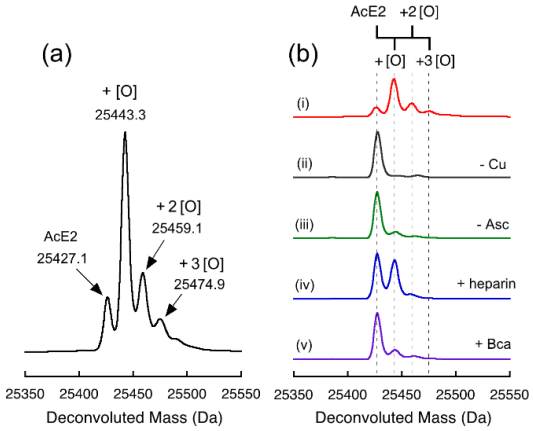

Figure 10. Oxidation of APP-E2 from the catalytic cycles shown in Figure 9a. (a) Deconvoluted mass spectrum of E2 (20 μM) following incubation with Cu(II) ions (5.0 μM) and reductant Asc (50 μM) for 1 hour in an aerobic Mops buffer. (b) Deconvoluted mass spectra of E2 show the extent of protein oxidation in solutions of varying compositions, as listed in Table 4.

Table 4. Aerobic oxidation of Asc catalysed by Cu-E2 complex in solutions of varying compositions

Expt in Figure 10b	Solution compositions (μM) [a]					Relative reaction rate[b]
	Cu	E2	heparin	Asc	Bca	
i	5	20	-	50	-	1.0
ii	-	20	-	50	-	0.01
iii	5	20	-	-	-	n/a
iv	5	20	20	50	-	0.44
v	5	20	-	50	25	0.05

[a] In Mops buffer (50 mM, pH 7.4, 100 mM NaCl); [b] relative to that of Expt (i).

DISCUSSION

Analysis of copper binding and reactivity in sAPPα and subdomains

Subdomains D1 and D2 of domain E1 of APP (Figure 1) bind Cu(II) with lower affinity (K_D ~ 10 nM) than Cu(I) (K_D ~ 0.1 nM).[39] Both feature bis-His binding sites, identified previously by X-ray crystallography.[37] Equivalent studies of E1 did not detect cooperativity in the binding (Figures 3 and 4).

More significantly, this study estimated a pM affinity for Cu(II) binding at pH 7.4 to the tetra-His M1 site in APP E2. This is the only high affinity Cu(II) binding site within the entire soluble ectodomain sAPPα (or the slightly shorter form sAPPβ).

In the presence of heparin, a pM affinity for Cu(I) binding to M1 (or a ligand subset) was defined recently.[40] In its absence, Cu(I) binding induced formation of a stable ternary complex E2-Cu(I)-L (L = probe ligand) that prevented quantification of the Cu(I) affinity.[40] The present work confirmed that these properties are retained in sAPPα and that the other Cu(I) binding sites of weaker affinities do not compete.

Heparin is known to promote APP dimerization[26, 32] and this is confirmed for isolated sAPPα (Figure S13). Because of the abundance of heparins and heparan sulfate proteoglycans in the extracellular matrix (ECM), these dimeric structures are likely to be the predominant forms of APP at the cell-surface.[33, 53] In intracellular compartments, APP co-localizes with the proteoglycan glypican-1 (Gpc-1)[54-55] and Cu-sAPPβ complexes may be involved in the Asc-induced cleavage of its heparin sulfate chains in endosomes as part of Gpc-1 recycling.[54, 56] Heparin binding sites have been identified in APP D1 and E2 domains (Figure 1), and they may be involved in APP's modulation of neurite formation.[55] That in D1 includes Cu binding residues H108 and H110, while that in E2 encompasses (and may directly involve) the M1 site.[57-58] Furthermore, coordination of metal ions, including Cu(II) and Zn(II), to the M1 site has been shown to enhance heparin binding in domain E2.[58] However, this work demonstrated that the impact of heparin on Cu(I) or Cu(II) binding to sAPPα or its subdomains is minimal (Table 2), although heparin is required for disruption of the ternary Cu(I) complex E2-Cu(I)-L discussed above.

Specific cellular conditions may promote interactions between copper and APP

Under conditions that mimic the extracellular space (pH 7.4, 100 mM NaCl), the M1 site in APP possesses a pM affinity for Cu(II) that is comparable to that of the extracellular domain (Ctr1n) of Ctr1, but is about an order of magnitude weaker than that of the ATCUN site of HSA (Table 2). The latter situation would appear to disfavor Cu-APP interactions. However, the M1 site can compete both thermodynamically (Figure 7) and kinetically (Figure S10) with HSA (and likely with Ctr1n as well) for Cu(II) binding at pH 7.4. In addition, Cu(II) bound in the M1 site can be reduced readily to Cu(I) by Asc (Figure 9b) but Cu(II) bound by an ATCUN site is generally redox inactive. These combined effects are expected to overcome the thermodynamic disadvantage of Cu(II) binding to the M1 site in the presence of HSA and to enhance interaction between Cu and APP at pH 7.4. This may be important at glutamatergic synapses where high concentrations of Cu are reportedly released.[59-61]

Notably, the Cu(I) affinities of the APP M1 site and the Ctr1n domain are both in the pM range (Table 2), providing the possibility of rapid exchange of Cu(I) between sAPPα (or sAPPβ) and Ctr1 in the extracellular space and a potential role in Cu homeostasis.[15-16]

It is important to consider the distribution of the protein between different cellular compartments (see Figure 11). A fraction of APP only resides at the cell surface (pH ~ 7.4) with the majority present in intracellular compartments including the endoplasmic reticulum (pH ~7.2), trans-Golgi network (pH ~6.5), endosomes (pH ~5.5-6.5) and lysosomes (pH ~4.7).[62-66] The different ambient pH in each environment may have a substantial impact on metal distribution. For example, this study revealed a shift of dominant Cu(II) binding from HSA to APP E2 upon lowering solution pH from 7.4 to 6.2 (Figures 6 and 7).

Furthermore, although the availability of free Cu in the cytoplasm is extremely low, intracellular Cu 'stores' may exist in other subcellular locations. For example, Ctr1 and its structural relative Ctr2 are involved in the mobilization of Cu from endosomal stores.[67-68] This process is regulated by cleavage of the large extracellular domain of Ctr1 (Ctr1n)[69] which binds both Cu(I) and Cu(II) with affinities comparable to those of the APP M1 site (Table 2). Consequently, Cu bioavailability in these compartments may approach the level required for APP E2 acquisition as well. Recent work suggests that the β-secretase BACE1 (which interacts with and cleaves APP in acidic compartments such as endosomes[66]) may be responsible for redistributing Cu ions from the cytoplasm to intracellular compartments.[70]

Implications for biological function and disease

Biological studies linking Cu and APP *in vivo* are summarized in Figure 11. The following assessment relates the known Cu chemistry of APP to its reported biological behavior.

ESI-MS (Figures 8, S11) corroborated X-ray crystallographic data[36] that indicated significant conformational changes in APP-E2 upon binding of Cu(II). Such changes may modulate APP function at synapses.[71] The protein is known to localize in synaptic clefts and significant concentrations of Cu are reportedly released there (see Figure 11a).[37, 59-61]

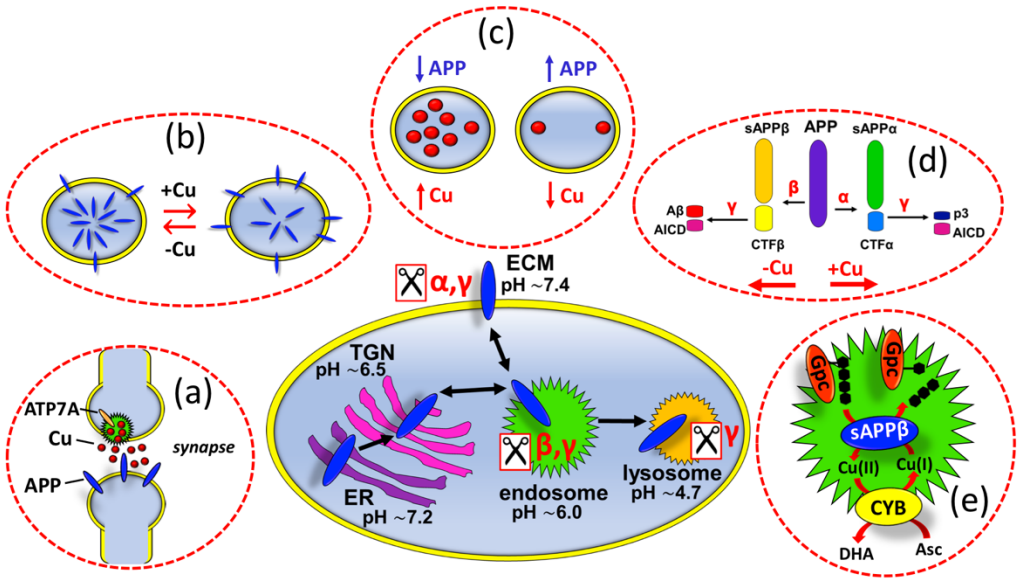

Figure 11. Potential biological implications of Cu-APP interactions in a range of subcellular locations. Central main figure: APP (blue ellipse) matures through the secretory pathway, from the endoplasmic reticulum (ER) to the trans-Golgi network (TGN) and is then transported to the plasma membrane via endosomal compartments. APP can be cleaved from the plasma membrane by α-secretase, releasing the soluble extracellular fragment sAPPα, or alternatively re-internalised into intracellular endosomal compartments and the TGN. A proportion is directed to lysosomal compartments for degradation. Proposed relationships between APP and Cu homeostasis *in vivo* include: (a) APP localises to synaptic sites[72] where significant Cu concentrations (red spheres) are released[60-61] that may modulate APP function at synapses (see refs [37, 73-75]); (b) Cu promotes trafficking of APP from intracellular compartments to the plasma membrane (see refs [21, 23]); (c) APP may play a role in Cu export: intracellular Cu levels are inversely proportional to APP expression levels (see refs [15, 76]); (d) Cu affects APP processing pathways: increased Cu levels promote non-amyloidogenic processing and Cu deficiency enhances amyloidogenic processing and Aβ production (see refs [10, 19-20]); (e) Cu-APP complexes may catalyse heparin sulfate (HS) cleavage from glypican-1 (Gpc) in endosomes: in the proposed model, ascorbate drives reductive deamination of HS via an electron transfer chain involving cytochrome b561 (CYB) and Cu-sAPPβ (see refs [54, 56]).

As suggested previously,[36] structural changes could also trigger Cu-promoted trafficking of APP (Figure 11b) by modulating interactions between APP and sorting proteins. However, we note that indirect effects, such as Cu-induced alterations to kinase pathways,[23, 77] may also be responsible for Cu-induced APP relocation. The proposed 'Cu export' function of APP[78] (Figure 11c) may be linked to this trafficking[21] as enhanced APP exocytosis could facilitate the release of Cu cargo from intracellular vesicles in a manner reminiscent of the actions of Cu-pumps ATP7A and ATP7B.[22] Likewise, because the α-, β- and γ-secretases are active in distinct cellular compartments[66], cellular redistribution of APP will affect its proteolytic processing. This is a possible explanation of the observed Cu-dependent changes in Aβ production (Figure 11d). Alternatively, Cu-APP interactions and resulting structural changes in domain E2 (which is adjacent to cleavage sites; see Figure 1) could directly affect APP processing.

The observed redox activity of the Cu-E2 complex and its ability to produce ROS is potentially related to both functional and pathogenic interactions of APP. It has been shown that Asc-driven cleavage of heparin sulfate chains from S-nitrosylated Gpc-1 in endosomes is dependent on both Cu and APP.[54, 56] The proposed mechanism involves the Cu complex of sAPPβ as a redox catalyst in the reductive deamination of heparin sulfate chains (Figure 11e). It was demonstrated in the present work that: (i) the thermodynamics of Cu-E2 binding interactions allows Cu to readily cycle between its two oxidation states and (ii) Asc-driven redox-cycling occurs *in vitro*, including when Cu-E2 is bound to heparin chains. This suggests that the Cu-E2 complex is a likely candidate for catalyzing heparin sulfate cleavage, particularly considering: (i) domain E2 contains the highest affinity heparin binding site in APP[53, 79] and (ii) coordination of Cu(II) further promotes E2-heparin interactions.[58] The heparin-binding site in E2 has been mapped to the region surrounding the M1 site,[57-58] thereby positioning redox-active Cu ions in close proximity to the reactive free thiols and heparin sulfate cleavage sites of Gpc-1. It is expected that, in this context, redox reactions involving Cu-APP species could be controlled and electrons directed specifically to the S-nitrosylated cysteines of Gpc-1 (thus facilitating release of NO^- and, subsequently, cleavage of heparin sulfate; see refs [56, 80-81]).

However, simple uncontrolled *in vitro* redox cycling of Cu-E2 can produce ROS and cause protein damage (Figure 10). This suggests that dysregulation of Cu-APP redox activity could potentially lead to oxidative damage (observed in AD brain tissues). Interestingly, the ternary complex between APP E2 and ligand Bca is a stable Cu(I) species which does not undergo re-

dox cycling in the presence of Asc and dioxygen (Table 4). Furthermore, such ternary complexes are disrupted by heparin binding to APP E2 (see ref [40] and Figure S6). Although Bca is not a biological molecule, it is reasonable to speculate that similar ternary complexes involving biological co-ligand(s) could form *in vivo* and that the interplay between ternary complex formation and heparin-binding could modulate the redox activity of Cu-APP species.

CONCLUSIONS

The primary conclusion is that, under copper limiting conditions, the M1 site in domain E2 dominates the properties of the entire APP ectodomain with comparable pM affinities for both oxidation states Cu(I) and Cu(II) (Table 2). The pH dependence of the apparent affinities, plus the redox activity of the bound copper, indicates that APP should compete for copper in a number of subcellular locations (Figure 11).

The site is redox-active under physiological conditions (Figure 9). Redox catalysis involving O_2 induced oxidation of the APP E2 protein itself (Figure 10), a common phenomenon in similar systems.[82]

There is significant uncertainty about the roles (natural or pathological) of Cu-APP interactions in the human brain and about when (conditions of copper availability) and where (in which subcellular locations) such interactions may occur. Identification of the highest affinity copper binding site in the ectodomain of APP (and its pH dependence) will guide experiments aimed at a molecular understanding of the significance of these interactions.

ASSOCIATED CONTENT

Supporting Information

The Supporting Information is available free of charge on the ACS Publications website. Details of experimental procedures; Tables S1-3; Figures S1-14 (PDF).

AUTHOR INFORMATION

Corresponding Author

* zhiguang.xiao@florey.edu.au

Notes

The authors declare no competing financial interest.

ACKNOWLEDGMENT

This work was supported by funds from the Australian Research Council Grant DP130100728. Additional financial support for TRY was generously provided by the Norma Hilda Schuster (née Swift) Scholarship Fund and the Albert Shimmins Fund. Part of ESI-MS analysis was conducted at the Bio21 Mass Spectrometry and Proteomics Facility. We thank Andrea Tester for technical assistance in protein expression in *Pichia pastoris* cells and Sioe See Volaric for technical assistance with EPR spectroscopy.

REFERENCES

1. Glenner, G. G.; Wong, C. W., Alzheimer's disease: initial report of the purification and characterization of a novel cerebrovascular amyloid protein. *Biochemical and biophysical research communications* **1984,** *120* (3), 885-90.
2. Kang, J.; Lemaire, H.-G.; Unterbeck, A.; Salbaum, J. M.; Masters, C. L.; Grzeschik, K.-H.; Multhaup, G.; Beyreuther, K.; Muller-Hill, B., The precursor of Alzheimer's disease amyloid A4 protein resembles a cell-surface receptor. *Nature* **1987,** *325* (6106), 733-736.
3. Muller, U. C.; Deller, T.; Korte, M., Not just amyloid: physiological functions of the amyloid precursor protein family. *Nature Reviews Neuroscience* **2017,** *18* (5), 281-298.
4. Kaden, D.; Bush, A. I.; Danzeisen, R.; Bayer, T. A.; Multhaup, G., Disturbed copper bioavailability in Alzheimer's disease. *Int J Alzheimers Dis* **2011,** *2011*, 345614.
5. Lovell, M. A.; Robertson, J. D.; Teesdale, W. J.; Campbell, J. L.; Markesbery, W. R., Copper, iron and zinc in Alzheimer's disease senile plaques. *Journal of the Neurological Sciences* **1998,** *158* (1), 47-52.
6. Miller, L. M.; Wang, Q.; Telivala, T. P.; Smith, R. J.; Lanzirotti, A.; Miklossy, J., Synchrotron-based infrared and X-ray imaging shows focalized accumulation of Cu and Zn co-localized with beta-amyloid deposits in Alzheimer's disease. *Journal of Structural Biology* **2006,** *155* (1), 30-7.
7. Deibel, M. A.; Ehmann, W. D.; Markesbery, W. R., Copper, iron, and zinc imbalances in severely degenerated brain regions in Alzheimer's disease: possible relation to oxidative stress. *Journal of the Neurological Sciences* **1996,** *143* (1-2), 137-42.
8. Magaki, S.; Raghavan, R.; Mueller, C.; Oberg, K. C.; Vinters, H. V.; Kirsch, W. M., Iron, copper, and iron regulatory protein 2 in Alzheimer's disease and related dementias. *Neuroscience Letters* **2007,** *418* (1), 72-76.
9. Hureau, C.; Faller, P., Aβ-mediated ROS production by Cu ions: Structural insights, mechanisms and relevance to Alzheimer's disease. *Biochimie* **2009,** *91* (10), 1212-1217.
10. Bayer, T. A.; Schafer, S.; Simons, A.; Kemmling, A.; Kamer, T.; Tepest, R.; Eckert, A.; Schussel, K.; Eikenberg, O.; Sturchler-Pierrat, C.; Abramowski, D.; Staufenbiel, M.; Multhaup, G., Dietary Cu stabilizes brain superoxide dismutase 1 activity and reduces amyloid Abeta production in APP23 transgenic mice. *Proceedings of the National Academy of Sciences of the United States of America* **2003,** *100* (24), 14187-92.
11. Duncan, C.; White, A. R., Copper complexes as therapeutic agents. *Metallomics* **2012,** *4* (2), 127-138.
12. Barnham, K. J.; Bush, A. I., Biological metals and metal-targeting compounds in major neurodegenerative diseases. *Chemical Society Reviews* **2014,** *43* (19), 6727-6749.
13. Sampson, E. L.; Jenagaratnam, L.; McShane, R., Metal protein attenuating compounds for the treatment of Alzheimer's dementia. *Cochrane Database of Systematic Reviews* **2014,** (2), CD005380.

14. Drew, S. C., The Case for Abandoning Therapeutic Chelation of Copper Ions in Alzheimer's Disease. *Frontiers in Neuroscience* **2017,** *11* (317), 317.
15. White, A. R.; Reyes, R.; Mercer, J. F.; Camakaris, J.; Zheng, H.; Bush, A. I.; Multhaup, G.; Beyreuther, K.; Masters, C. L.; Cappai, R., Copper levels are increased in the cerebral cortex and liver of APP and APLP2 knockout mice. *Brain Research* **1999,** *842* (2), 439-44.
16. Bellingham, S. A.; Ciccotosto, G. D.; Needham, B. E.; Fodero, L. R.; White, A. R.; Masters, C. L.; Cappai, R.; Camakaris, J., Gene knockout of amyloid precursor protein and amyloid precursor-like protein-2 increases cellular copper levels in primary mouse cortical neurons and embryonic fibroblasts. *Journal of Neurochemistry* **2004,** *91* (2), 423-8.
17. Bellingham, S. A.; Lahiri, D. K.; Maloney, B.; La Fontaine, S.; Multhaup, G.; Camakaris, J., Copper depletion down-regulates expression of the Alzheimer's disease amyloid-beta precursor protein gene. *Journal of Biological Chemistry* **2004,** *279* (19), 20378-86.
18. Armendariz, A. D.; Gonzalez, M.; Loguinov, A. V.; Vulpe, C. D., Gene expression profiling in chronic copper overload reveals upregulation of Prnp and App. *Physiological Genomics* **2004,** *20* (1), 45-54.
19. Borchardt, T.; Camakaris, J.; Cappai, R.; Masters, C. L.; Beyreuther, K.; Multhaup, G., Copper inhibits beta-amyloid production and stimulates the non-amyloidogenic pathway of amyloid-precursor-protein secretion. *Biochemical Journal* **1999,** *344 Pt 2*, 461-7.
20. Cater, M. A.; McInnes, K. T.; Li, Q. X.; Volitakis, I.; La Fontaine, S.; Mercer, J. F.; Bush, A. I., Intracellular copper deficiency increases amyloid-beta secretion by diverse mechanisms. *Biochemical Journal* **2008,** *412* (1), 141-52.
21. Acevedo, K. M.; Hung, Y. H.; Dalziel, A. H.; Li, Q. X.; Laughton, K.; Wikhe, K.; Rembach, A.; Roberts, B.; Masters, C. L.; Bush, A. I.; Camakaris, J., Copper promotes the trafficking of the amyloid precursor protein. *Journal of Biological Chemistry* **2011,** *286* (10), 8252-62.
22. Petris, M. J.; Mercer, J. F.; Culvenor, J. G.; Lockhart, P.; Gleeson, P. A.; Camakaris, J., Ligand-regulated transport of the Menkes copper P-type ATPase efflux pump from the Golgi apparatus to the plasma membrane: a novel mechanism of regulated trafficking. *EMBO Journal* **1996,** *15* (22), 6084-6095.
23. Acevedo, K. M.; Opazo, C. M.; Norrish, D.; Challis, L. M.; Li, Q.-X.; White, A. R.; Bush, A. I.; Camakaris, J., Phosphorylation of amyloid precursor protein at threonine 668 is essential for its copper-responsive trafficking in SH-SY5Y neuroblastoma cells. *Journal of Biological Chemistry* **2014,** *289* (16), 11007-11019.
24. Rossjohn, J.; Cappai, R.; Feil, S. C.; Henry, A.; McKinstry, W. J.; Galatis, D.; Hesse, L.; Multhaup, G.; Beyreuther, K.; Masters, C. L.; Parker, M. W., Crystal structure of the N-terminal, growth factor-like domain of Alzheimer amyloid precursor protein. *Nature Structural Biology* **1999,** *6* (4), 327-331.
25. Barnham, K. J.; McKinstry, W. J.; Multhaup, G.; Galatis, D.; Morton, C. J.; Curtain, C. C.; Williamson, N. A.; White, A. R.; Hinds, M. G.; Norton, R. S.; Beyreuther, K.; Masters, C. L.; Parker, M. W.; Cappai, R., Structure of the Alzheimer's disease amyloid precursor protein copper binding domain. A regulator of neuronal copper homeostasis. *Journal of Biological Chemistry* **2003,** *278* (19), 17401-7.
26. Dahms, S. O.; Hoefgen, S.; Roeser, D.; Schlott, B.; Gührs, K.-H.; Than, M. E., Structure and biochemical analysis of the heparin-induced E1 dimer of the amyloid precursor protein. *Proceedings of the National Academy of Sciences* **2010,** *107* (12), 5381-5386.
27. Dawkins, E.; Small, D. H., Insights into the physiological function of the β - amyloid precursor protein: beyond Alzheimer's disease. *Journal of Neurochemistry* **2014,** *129* (5), 756-769.
28. Small, D. H.; Nurcombe, V.; Reed, G.; Clarris, H.; Moir, R.; Beyreuther, K.; Masters, C. L., A heparin-binding domain in the amyloid protein precursor of Alzheimer's disease is involved in the regulation of neurite outgrowth. *Journal of Neuroscience* **1994,** *14* (4), 2117-2127.
29. Multhaup, G., Identification and regulation of the high affinity binding site of the Alzheimer's disease amyloid protein precursor (APP) to glycosaminoglycans. *Biochimie* **1994,** *76* (3), 304-311.
30. Clarris, H. J.; Cappai, R.; Heffernan, D.; Beyreuther, K.; Masters, C. L.; Small, D. H., Identification of Heparin-Binding Domains in the Amyloid Precursor Protein of Alzheimer's Disease by Deletion Mutagenesis and Peptide Mapping. *Journal of Neurochemistry* **1997,** *68* (3), 1164-1172.
31. Williamson, T. G.; Nurcombe, V.; Beyreuther, K.; Masters, C. L.; Small, D. H., Affinity Purification of Proteoglycans that Bind to the Amyloid Protein Precursor of Alzheimer's Disease. *Journal of Neurochemistry* **1995,** *65* (5), 2201-2208.
32. Gralle, M.; Oliveira, C. L. P.; Guerreiro, L. H.; McKinstry, W. J.; Galatis, D.; Masters, C. L.; Cappai, R.; Parker, M. W.; Ramos, C. H. I.; Torriani, I.; Ferreira, S. T., Solution Conformation and Heparin-induced Dimerization of the Full-length Extracellular Domain of the Human Amyloid Precursor Protein. *Journal of Molecular Biology* **2006,** *357* (2), 493-508.
33. Gralle, M.; Botelho, M. G.; Wouters, F. S., Neuroprotective Secreted Amyloid Precursor Protein Acts by Disrupting Amyloid Precursor Protein Dimers. *Journal of Biological Chemistry* **2009,** *284* (22), 15016-15025.
34. Sosa, L. J.; Cáceres, A.; Dupraz, S.; Oksdath, M.; Quiroga, S.; Lorenzo, A., The physiological role of the amyloid precursor protein as an adhesion molecule in the developing nervous system. *Journal of Neurochemistry* **2017,** *143* (1), 11-29.
35. Kong, G. K.; Adams, J. J.; Harris, H. H.; Boas, J. F.; Curtain, C. C.; Galatis, D.; Masters, C. L.; Barnham, K. J.; McKinstry, W. J.; Cappai, R.; Parker, M. W., Structural Studies of the Alzheimer's Amyloid Precursor Protein

Copper-binding Domain Reveal How it Binds Copper Ions. *Journal of Molecular Biology* **2007,** *367* (1), 148-61.
36. Dahms, S. O.; Könnig, I.; Roeser, D.; Gührs, K.-H.; Mayer, M. C.; Kaden, D.; Multhaup, G.; Than, M. E., Metal Binding Dictates Conformation and Function of the Amyloid Precursor Protein (APP) E2 Domain. *Journal of Molecular Biology* **2012,** *416* (3), 438-452.
37. Baumkötter, F.; Schmidt, N.; Vargas, C.; Schilling, S.; Weber, R.; Wagner, K.; Fiedler, S.; Klug, W.; Radzimanowski, J.; Nickolaus, S., Amyloid Precursor Protein Dimerization and Synaptogenic Function Depend on Copper Binding to the Growth Factor-Like Domain. *Journal of Neuroscience* **2014,** *34* (33), 11159-11172.
38. Hesse, L.; Beher, D.; Masters, C. L.; Multhaup, G., The beta A4 amyloid precursor protein binding to copper. *FEBS letters* **1994,** *349* (1), 109-16.
39. Leong, S. L.; Young, T. R.; Barnham, K. J.; Wedd, A. G.; Hinds, M. G.; Xiao, Z.; Cappai, R., Quantification of Copper Binding to Amyloid Precursor Protein Domain 2 and its *Caenorhabditas elegans* Ortholog. Implications for Biological Function. *Metallomics* **2013,** *6*, 105-16.
40. Young, T. R.; Wedd, A. G.; Xiao, Z., Evaluation of Cu(i) binding to the E2 domain of the amyloid precursor protein - a lesson in quantification of metal binding to proteins via ligand competition. *Metallomics* **2018,** *10* (1), 108-119.
41. Xiao, Z.; Gottschlich, L.; Meulen, R. V. D.; Udagedara, S. R.; Wedd, A. G., Evaluation of Quantitative Probes for Weaker Cu(I) Binding Sites Completes a Set of Four Capable of Detecting Cu(I) Affinities from Nanomolar to Attomolar. *Metallomics* **2013,** *5*, 501-513.
42. Young, T. R.; Wijekoon, C. J. K.; Spyrou, B.; Donnelly, P. S.; Wedd, A. G.; Xiao, Z., A set of robust fluorescent peptide probes for quantification of Cu(ii) binding affinities in the micromolar to femtomolar range. *Metallomics* **2015,** *7* (3), 567-578.
43. Xiao, Z.; Brose, J.; Schimo, S.; Ackland, S. M.; La Fontaine, S.; Wedd, A. G., Unification of the copper(I) binding affinities of the metallo-chaperones Atx1, Atox1 and related proteins: detection probes and affinity standards. *J Biol Chem* **2011,** *286* (13), 11047-11055.
44. Likely another one comprising two adjacent His residues in the C-terminus of the un-cleaved Aβ16 sequence (see the protein sequence in Figure S3).
45. Rózga, M.; Sokołowska, M.; Protas, A. M.; Bal, W., Human serum albumin coordinates Cu(II) at its N-terminal binding site with 1 pM affinity. *Journal of Biological Inorganic Chemistry* **2007,** *12* (6), 913-918.
46. Haas, K. L.; Putterman, A. B.; White, D. R.; Thiele, D. J.; Franz, K. J., Model Peptides Provide New Insights into the Role of Histidine Residues as Potential Ligands in Human Cellular Copper Acquisition via Ctr1. *Journal of the American Chemical Society* **2011,** *133* (12), 4427-4437.
47. Wijekoon, C. J. K.; Young, T. R.; Wedd, A. G.; Xiao, Z., The CopC Protein from Pseudomonas fluorescens SBW25 Features A Conserved Novel High Affinity Cu(II) Binding Site. *Inorganic Chemistry* **2015,** *54* (6), 2950-2959.
48. Leney, A. C.; Heck, A. J. R., Native Mass Spectrometry: What is in the Name? *Journal of the American Society for Mass Spectrometry* **2017,** *28* (1), 5-13.
49. Ruotolo, B. T.; Benesch, J. L. P.; Sandercock, A. M.; Hyung, S.-J.; Robinson, C. V., Ion mobility-mass spectrometry analysis of large protein complexes. *Nat. Protocols* **2008,** *3* (7), 1139-1152.
50. Conway, B., Electrochemical Data. Greenwood Press New York, 1969.
51. Nelson, D. L.; Lehninger, A. L.; Cox, M. M., *Lehninger principles of biochemistry*. Macmillan: 2008.
52. Rice, M. E., Ascorbate regulation and its neuroprotective role in the brain. *Trends Neurosci.* **2000,** *23* (5), 209-216.
53. Hoefgen, S.; Coburger, I.; Roeser, D.; Schaub, Y.; Dahms, S. O.; Than, M. E., Heparin induced dimerization of APP is primarily mediated by E1 and regulated by its acidic domain. *Journal of Structural Biology* **2014,** *187* (1), 30-37.
54. Cappai, R.; Cheng, F.; Ciccotosto, G. D.; Needham, B. E.; Masters, C. L.; Multhaup, G.; Fransson, L.-Å.; Mani, K., The amyloid precursor protein (APP) of Alzheimer disease and its paralog, APLP2, modulate the Cu/Zn-Nitric Oxide-catalyzed degradation of glypican-1 heparan sulfate in vivo. *Journal of Biological Chemistry* **2005,** *280* (14), 13913-13920.
55. Williamson, T. G.; San Mok, S.; Henry, A.; Cappai, R.; Lander, A. D.; Nurcombe, V.; Beyreuther, K.; Masters, C. L.; Small, D. H., Secreted glypican binds to the amyloid precursor protein of Alzheimer's disease (APP) and inhibits APP-induced neurite outgrowth. *Journal of Biological Chemistry* **1996,** *271* (49), 31215-31221.
56. Cheng, F.; Fransson, L.-Å.; Mani, K., Cytochrome b561, copper, β-cleaved amyloid precursor protein and niemann-pick C1 protein are involved in ascorbate-induced release and membrane penetration of heparan sulfate from endosomal S-nitrosylated glypican-1. *Experimental Cell Research* **2017,** *360* (2), 171-179.
57. Xue, Y.; Lee, S.-W.; Wang, Y.-C.; Ha, Y., Crystal Structure of the E2 Domain of Amyloid Precursor Protein-like Protein 1 in Complex with Sucrose Octasulfate. *Journal of Biological Chemistry* **2011,** *286* (Copyright (C) 2014 American Chemical Society (ACS). All Rights Reserved.), 29748-29757.
58. Dienemann, C.; Coburger, I.; Mehmedbasic, A.; Andersen, O. M.; Than, M. E., Mutants of the metal binding site M1 in APP-E2 show metal-specific differences in binding of heparin but not of sorLA. *Biochemistry* **2015,** *54*, 2490-2499.
59. Kardos, J.; Kovács, I.; Hajós, F.; Kálmán, M.; Simonyi, M., Nerve endings from rat brain tissue release copper upon depolarization. A possible role in regulating neuronal excitability. *Neuroscience Letters* **1989,** *103* (2), 139-144.
60. Schlief, M. L.; Craig, A. M.; Gitlin, J. D., NMDA Receptor Activation Mediates Copper Homeostasis in Hippocampal Neurons. *Journal of Neuroscience* **2005,** *25* (1), 239-246.

61. Schlief, M. L.; Gitlin, J. D., Copper homeostasis in the CNS. *Molecular Neurobiology* **2006,** *33* (2), 81-90.
62. Llopis, J.; McCaffery, J. M.; Miyawaki, A.; Farquhar, M. G.; Tsien, R. Y., Measurement of cytosolic, mitochondrial, and Golgi pH in single living cells with green fluorescent proteins. *Proceedings of the National Academy of Sciences of the United States of America* **1998,** *95* (12), 6803-6808.
63. Wu, M. M.; Llopis, J.; Adams, S.; McCaffery, J. M.; Kulomaa, M. S.; Machen, T. E.; Moore, H.-P. H.; Tsien, R. Y., Organelle pH studies using targeted avidin and fluorescein–biotin. *Chemistry & Biology* **2000,** *7* (3), 197-209.
64. Kaden, D.; Voigt, P.; Munter, L.-M.; Bobowski, K. D.; Schaefer, M.; Multhaup, G., Subcellular localization and dimerization of APLP1 are strikingly different from APP and APLP2. *Journal of Cell Science* **2009,** *122* (3), 368-377.
65. Casey, J. R.; Grinstein, S.; Orlowski, J., Sensors and regulators of intracellular pH. *Nature Reviews Molecular Cell Biology* **2010,** *11* (1), 50-61.
66. Haass, C.; Kaether, C.; Thinakaran, G.; Sisodia, S., Trafficking and proteolytic processing of APP. *Cold Spring Harbor perspectives in medicine* **2012,** *2* (5), a006270.
67. van den Berghe, P V. E.; Folmer, D E.; Malingré, H E. M.; van Beurden, E.; Klomp, Adriana E. M.; van de Sluis, B.; Merkx, M.; Berger, R.; Klomp, L W. J., Human copper transporter 2 is localized in late endosomes and lysosomes and facilitates cellular copper uptake. *Biochemical Journal* **2007,** *407* (1), 49-59.
68. Öhrvik, H.; Nose, Y.; Wood, L. K.; Kim, B.-E.; Gleber, S.-C.; Ralle, M.; Thiele, D. J., Ctr2 regulates biogenesis of a cleaved form of mammalian Ctr1 metal transporter lacking the copper-and cisplatin-binding ecto-domain. *Proceedings of the National Academy of Sciences* **2013,** *110* (46), E4279-E4288.
69. Öhrvik, H.; Logeman, B.; Turk, B.; Reinheckel, T.; Thiele, D. J., Cathepsin Protease Controls Copper and Cisplatin Accumulation via Cleavage of the Ctr1 Metal-binding Ectodomain. *Journal of Biological Chemistry* **2016,** *291* (27), 13905-13916.
70. Liebsch, F.; Aurousseau, M. R. P.; Bethge, T.; McGuire, H.; Scolari, S.; Herrmann, A.; Blunck, R.; Bowie, D.; Multhaup, G., Full-length cellular β-secretase has a trimeric subunit stoichiometry, and its sulfur-rich transmembrane interaction site modulates cytosolic copper compartmentalization. *Journal of Biological Chemistry* **2017,** *292* (32), 13258-13270.
71. Ludewig, S.; Korte, M., Novel Insights into the Physiological Function of the APP (Gene) Family and Its Proteolytic Fragments in Synaptic Plasticity. *Frontiers in Molecular Neuroscience* **2017,** *9*, 161.
72. Schubert, W.; Prior, R.; Weidemann, A.; Dircksen, H.; Multhaup, G.; Masters, C. L.; Beyreuther, K., Localization of Alzheimer βA4 amyloid precursor protein at central and peripheral synaptic sites. *Brain Research* **1991,** *563* (1), 184-194.
73. Gaier, E. D.; Eipper, B. A.; Mains, R. E., Copper signaling in the mammalian nervous system: synaptic effects. *Journal of Neuroscience Research* **2013,** *91* (1), 2-19.
74. D'Ambrosi, N.; Rossi, L., Copper at synapse: Release, binding and modulation of neurotransmission. *Neurochemistry International* **2015,** *90*, 36-45.
75. Wild, K.; August, A.; Pietrzik, C. U.; Kins, S., Structure and Synaptic Function of Metal Binding to the Amyloid Precursor Protein and its Proteolytic Fragments. *Frontiers in Molecular Neuroscience* **2017,** *10* (21), 21.
76. Maynard, C. J.; Cappai, R.; Volitakis, I.; Cherny, R. A.; White, A. R.; Beyreuther, K.; Masters, C. L.; Bush, A. I.; Li, Q. X., Overexpression of Alzheimer's disease amyloid-beta opposes the age-dependent elevations of brain copper and iron. *Journal of Biological Chemistry* **2002,** *277* (47), 44670-6.
77. Crouch, P. J.; Hung, L. W.; Adlard, P. A.; Cortes, M.; Lal, V.; Filiz, G.; Perez, K. A.; Nurjono, M.; Caragounis, A.; Du, T.; Laughton, K.; Volitakis, I.; Bush, A. I.; Li, Q.-X.; Masters, C. L.; Cappai, R.; Cherny, R. A.; Donnelly, P. S.; White, A. R.; Barnham, K. J., Increasing Cu bioavailability inhibits Aβ oligomers and tau phosphorylation. *Proceedings of the National Academy of Sciences* **2009,** *106* (2), 381-386.
78. Treiber, C.; Simons, A.; Strauss, M.; Hafner, M.; Cappai, R.; Bayer, T. A.; Multhaup, G., Clioquinol mediates copper uptake and counteracts copper efflux activities of the amyloid precursor protein of Alzheimer's disease. *Journal of Biological Chemistry* **2004,** *279* (50), 51958-64.
79. San Mok, S.; Sberna, G.; Heffernan, D.; Cappai, R.; Galatis, D.; Clarris, H. J.; Sawyer, W. H.; Beyreuther, K.; Masters, C. L.; Small, D. H., Expression and analysis of heparin-binding regions of the amyloid precursor protein of Alzheimer's disease. *FEBS letters* **1997,** *415* (3), 303-307.
80. Mani, K.; Cheng, F.; Havsmark, B.; Jönsson, M.; Belting, M.; Fransson, L.-Å., Prion, Amyloid β-derived Cu(II) Ions, or Free Zn(II) Ions Support S-Nitroso-dependent Autocleavage of Glypican-1 Heparan Sulfate. *Journal of Biological Chemistry* **2003,** *278* (40), 38956-38965.
81. Cheng, F.; Svensson, G.; Fransson, L.-Å.; Mani, K., Non-conserved, S-nitrosylated cysteines in glypican-1 react with N-unsubstituted glucosamines in heparan sulfate and catalyze deaminative cleavage. *Glycobiology* **2012,** *22* (11), 1480-1486.
82. Cheignon, C.; Tomas, M.; Bonnefont-Rousselot, D.; Faller, P.; Hureau, C.; Collin, F., Oxidative stress and the amyloid beta peptide in Alzheimer's disease. *Redox Biol* **2018,** *14*, 450-464.